Screening model of metallic nonideal contacts in the integer quantized Hall regime

D. Eksi,[1] O. Kilicoglu,[1] O. Göktas,[2] and A. Siddiki[3,4]
[1]*Department of Physics, Trakya University, 22030 Edirne, Turkey*
[2]*Braun Center for Submicron Research, Department of Condensed Matter Physics, Weizmann Institute of Science, Rehovot 76100, Israel*
[3]*Physics Department, Faculty of Sciences, Istanbul University, 34134 Vezneciler, Istanbul, Turkey*
[4]*Physics Department, Harvard University, Cambridge, Massachusetts 02138, USA*
(Received 30 March 2010; revised manuscript received 27 July 2010; published 6 October 2010)

In this work, we calculate the electron and the current-density distributions both at the edges and the bulk of a two-dimensional electron system, focusing on ideal and nonideal contacts. A three-dimensional Poisson equation is solved self-consistently to obtain the potential profile in the absence of an external magnetic field considering a Hall bar defined both by gates (contacts) and etching (lateral confinement). In the presence of a perpendicular magnetic field, we obtain the spatial distribution of the incompressible strips, taking into account the electron-electron interactions within the Thomas-Fermi approximation. Using a local version of Ohm's law, together with a relevant conductivity model, we also calculate the current distribution. We observe that the incompressible strips can reside either on the edge or at the bulk depending on the field strength. Our numerical results show that, due to a density poor region just in front of the contacts, the incompressible strips are not in direct contact with the injection region when considering nonideal contact configuration. Such a nonideal contact is in strong contrast with the conventional edge channel pictures, hence has a strong influence on transport. We also take into account heating effects in a phenomenological manner and propose a current injection mechanism from the compressible regions to the incompressible regions. The model presented here perfectly agrees with the local probe experiments all together with the formation of hot-spots.

DOI: 10.1103/PhysRevB.82.165308 PACS number(s): 73.23.Ad, 73.43.−f

I. INTRODUCTION

Regardless of what system one is interested in theoretically, the metallic contacts deposited on the two-dimensional electron systems (2DESs) are the most important ingredients of the measurement, both experimentally[1–5] and theoretically.[6–9] Here, contacts are both the injection/collector and probe contacts. In a standard Hall experiment (not necessarily quantized) a perpendicular external magnetic field B is applied to the normal of the 2DES. The excess electrons are injected from the source contact and are collected at the drain contact by applying a finite potential difference between these two contacts. Meanwhile, one measures the (electrochemical) potential difference either between the contacts along the sample (longitudinal potential difference V_l measured between A1-A2 or B1-B2 in Fig. 1) or across the sample, the Hall potential V_H (measured between A1-B1 or A2-B2 in Fig. 1). Determining the actual contact resistances of each element is a cumbersome matter. Experimentally, the usual way of obtaining the (nonideal) contact resistance is the transmission line method, which gives an average approximate value by measuring a set of contacts defined on a stripe of mesa containing 2DES.[10] However, in the quantized Hall regime the determination of contact resistances becomes somewhat easier, since one *a priori* knows that the longitudinal resistance should vanish and Hall resistance is quantized to an integer submultiple of the von Klitzing constant $R_K=h/e^2=25\,812.807\,449(86)\ \Omega$ where e is the elementary charge and h is the Planck constant.[11]

The term nonideal contact stands for a case where the edge channels do not equilibrate at the contacts, hence reflection (or transmission) from channel to contact (or vice versa) is nonzero (not unity). In contrary, in an ideal contact *all* the channels are in equilibrium with the contacts, and reflection is zero. We should also clarify the notation *ideal Ohmic contact*: This term stands for a contact with finite resistance R_C, however, still obey the Ohm's law $V=IR_C$ where the applied current is I. Hence, a nonideal contact for the Landauer-Büttiker formalism, i.e., nonzero reflection, can still be an ideal Ohmic contact.[7] Since different terminologies are used to describe the contacts, we find useful to give the definitions as follows: (i) "ideal/nonideal" contacts are "reflectiveless/reflective" contacts in Büttiker formalism. Note that, alloyed contacts creating potential fluctuations are always nonideal and an ideal contact should satisfy the flat band condition. (ii) "Bad/good" contacts are very "high/low"-resistive contacts, or called notworking/working contacts. The reference is the sample resistance: in order to measure the sample properties in two-terminal measurement, the good contact has a low resistance with respect to the sample resistance, i.e., the potential drops mainly at the sample area and a small amount at the contact area. This potential drop at the contacts can be Ohmic (I-V linear). However, it is not important if it is negligible small in respect to the potential drop across the sample. The bad contacts usually have a huge resistance (a few tens of kilohm) which shadows the sample properties and it is difficult to pass the current through. Later, we also discuss the two types of contacts: The contact with the homogeneous/inhomogeneous density gradient, which present low/very-high resistances. Under magnetic field, they have very different properties. In the first case, the bulk and edge decouples from each other, meanwhile in the second case the bulk and edge are coupled.

It is a formidable task to model the sudden change in the density of states (DOS) near the contacts. Since, the DOS at the metallic region is approximately infinite, whereas at the

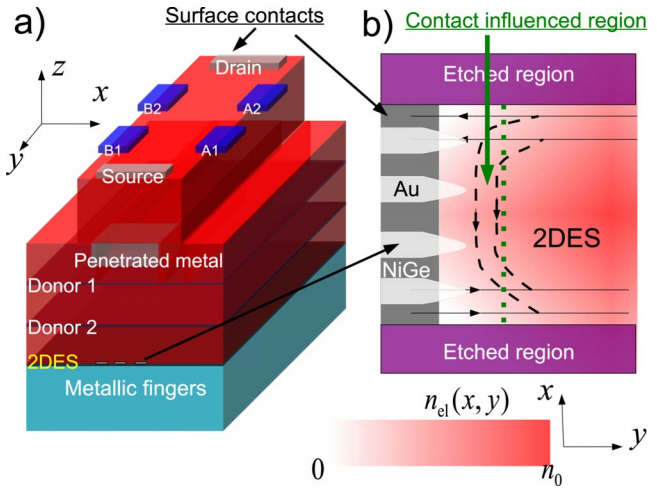

FIG. 1. (Color online) Schematic presentation of the Hall bar and contacts induced on a 3D GaAs/AlGaAs (red and blue regions) heterostructure (a). The sample has the dimensions of $1.5\times1.5\times0.85$ μm^3, mapped on a matrix of $96\times96\times110$ embedded in a dielectric material, where open boundary conditions are assumed on the border of the dielectric material. Two donor layers, distributed homogeneously on the *xy* plane, provide electrons both to surface and to the 2DES. Contacts are modeled by (i) a metallic gate on the surface, (ii) a metallic region inside the crystal, and (iii) fingers at the plane of 2DES, where fingers are to simulate bad contacts. (b) A sketch of 2D projection of the Hall bar from top: dark (gray and light gray) regions depict the contact, whereas the lateral confinement is shown by the etched regions. Color gradient represents the electron density, together with Landauer-Büttiker edge states, in the case of an ideal contact (straight lines) and a nonideal contact (broken curves).

2D system the DOS is a constant in the absence of an external magnetic field B. More interestingly, in the presence of B field the DOS varies as a function of energy, presenting maxima at the Landau energies and zeros between them. If there are no states available at the Fermi energy E_F the system is called incompressible,[12–14] otherwise compressible with high DOS at E_F. A very comprehensive review is provided in Ref. 6 discussing the properties of the contacts in terms of DOS without B field. Recently, there were numerical efforts to model the contacts by methods similar that of molecular dynamics[8] considering interacting classical electrons. The classical Hall potential distribution is obtained calculating actual forces (Lorentz and electrostatic), utilizing graphics processing units and many-body algorithms. The ideal contacts are modeled as equipotential surfaces, where no density poor region resides just in front of the contacts. Whereas, the nonideal contacts were described by different injection probabilities at the injection region. In this work, the density fluctuations near the contact/GaAs interface is left unresolved, which influences the current distribution drastically as shown by the experiments.[2,5] An important drawback of this approach is, it cannot handle quantum mechanical effects with its present form, therefore cannot account for the integer quantized Hall effect. Moreover, the experimental parameters used (e.g., the dielectric constant ϵ is taken as 8, however, it is as large as 50%) are not the typical parameters resembling the real systems. As a final remark, in experiments the electrons are not injected to an *empty* sample, where the Hall potential develops. Instead, the electronic system is in equilibrium before the current is injected, where electrostatic interactions already screened the external potential. Another recent work is reported by Oswald and co-workers[9] considering the nonequilibrium network model. In their analysis they show that the nonideal contacts have strong influence on the measured Hall resistance R_H and the longitudinal resistance R_l. The nonequilibrium network model disregards the interaction effects and calculates the electrochemical potential distribution by obtaining the transmission coefficients depending on the magnetic fields and given electrostatic potential.

In this paper, we present our self-consistently calculated results which takes into account Landau quantization and direct Coulomb interactions at a mean-field approximation level.[15,16] We investigate theoretically the current and charge-density distributions considering quantizing high B fields and intermediate electron-density concentrations (5×10^{10} $cm^{-2}<n_{el}<3\times10^{11}$ cm^{-2}) in the close proximity of the contacts, together with the entire sample. Our results point that, the assumption of ideal contacts cannot be justified, when considering *regular* density inhomogeneities which always exist in all low resistive alloyed contacts. We also take into account Joule heating following the lines of Akera and his co-workers,[17,18] phenomenologically and propose a self-consistent mechanism to inject current from compressible to incompressible regions (and vice versa). Our treatment of the contact regions is essentially based on the experimental findings of Weis and his co-workers, namely, scanning force microscopy experiments by Ahlswede[2] and comprehensive structural investigation by Dahlem[19] and Goektas.[5] Up to our knowledge, no comprehensive theoretical study of contacts is accessible in the literature that both take into account interactions, device geometry, potential fluctuations, and formation of incompressible and compressible regions, which exist due to Landau quantization. In Sec. II, we briefly summarize the basics of our numerical algorithms, where we first introduce the fourth-order grid method to solve the Poisson equation in three-dimensional (3D) to obtain the electrostatic quantities of the sample at hand. Next, we represent the self-consistent equations to calculate the electron-density, potential, and current distributions in the presence of a quantizing magnetic field. In Sec. III, we utilize the methods introduced in the previous sections to investigate the influence of contacts on the current distribution, also considering bad contacts. There, we show that the Landauer-Büttiker-type edge states are not in equilibrium with the contacts due to the density poor region in front of the metallic regions, unless the Landau levels are pinned to the Fermi energy due to special geometric conditions. We finalize our paper by a conclusion section.

II. SELF-CONSISTENT NUMERICAL ALGORITHMS

Describing the electrostatics of a semiconductor heterojunction in the quantum mechanical domain requires the self-consistent solutions of the Poisson and the Schrödinger equations in three dimensions. In principle, such a calculation is

possible with a very few number of particles (up to 10–15 electrons) and considering relatively small sample sizes (~100–200 nm, in all three directions). However, due to the computational limitations it is more or less impossible for realistic samples. The restriction results from the fact that one should span the Hilbert space of the electrons with sufficiently many wave functions and also the real (or momentum) space of the material in 3D. To reduce the computational effort, one can first solve the Poisson equation in 3D self-consistently assuming classical particles, namely, performing a mean-field Thomas-Fermi approximation. The solution of the Poisson equation, by imposing certain boundary conditions to be determined later, is of the form

$$V(x,y,z) = V_{\mathrm{ch}}(x,y,z) + V_{\mathrm{G}(x,y,z)} + V_{\mathrm{surf}}(x,y,z), \qquad (1)$$

where the first term accounts for the potential generated by the charges, the second for the gates, and the third for the surface potentials. Now, if the initial potentials are known one can obtain the charge distributions by

$$n_{\mathrm{ch}}(x,y,z) = \int dED(E)f[E,V(x,y,z),T] \qquad (2)$$

with the relevant DOS $D(E)$ and Fermi occupation function $f[E,V(x,y,z),T]$. In the following sections we will specify our boundary conditions, relevant density of states, and the properties of the charges.

In Ref. 5 it was pointed that a model which also takes into account the density gradient in front of the contacts is crucial in understanding the quantized Hall effect, especially when considering high perpendicular magnetic fields, where compressible and incompressible strips form. In this section, we present such a model by solving the Poisson equation in 3D self-consistently to obtain potential and charge-density distributions near the contact, together with the entire sample, employing a fourth-order grid technique.[15,20] In the next step we use the potential profile obtained at the plane of 2DES as an initial condition to calculate same quantities in the presence of a perpendicular B field. Our calculation scheme is based on a mean-field Thomas Fermi approximation improved by spatial course-graining to simulate quantum mechanical effects, such as the finite extent of the wave functions.[21] At a last step we impose a fixed current in y direction and calculate the current distribution utilizing a local version of the Ohm's law.[22] Here, we assume that the DOS and the temperature of electrons do not vary considerably on the quantum mechanical length scales, i.e., these quantities are position independent. The conductivity model is obtained from the self-consistent Born approximation[21,23] and local conductances are assumed to be directly related with the local electron density. Such an approximation can be considered as first order, however, is valid if the charge density changes slowly on the correlation length of the remote impurities.[24] An improved calculation scheme of the conductivities[25] already supports our assumptions related to the conductivity model. At the last part of this section we will address the limitations and validity regimes of such a transport model. Moreover, our results are independent of the choice of the particular conductivity model since we are not interested in the details of plateau to plateau transition regions. The only necessary ingredient of our conductivity model is to have vanishing (in fact exponentially small, at zero temperature) longitudinal conductance σ_l at incompressible regions and a Hall conductance σ_H proportional to the electron density. The last requirement also implies that, the Hall conductance is quantized at the incompressible regions.

A. 3D lattice without magnetic field

As mentioned above, the charge and potential distributions of the crystal has to be mapped on a 3D matrix which spans the system. The first step is to fix the boundary conditions: we assume that the system is embedded in a dielectric material with a dielectric constant of air. The potential satisfies the open boundary conditions, namely, $V(x,y,z)\to 0$ at $x,y,z\to\pm\infty$. Next we fix the positions of the positive charges (the donors) and the plane that the 2DES resides. Both are motivated by physical constraints, such that the ions are not mobile and one can ignore the finite thickness of the quantum well (~5–10 nm) in the z direction, when compared to the crystal size which is at the order of micrometers. Note also that the $D(E)$ at the interface is just a constant. We also impose that the surface potential of the crystal is kept constant since the Fermi energy is pinned to the midgap of the top-lying material in equilibrium, whereas the potentials at the metallic gates are to be given depending on the experimental conditions. At zero temperature and imposing charge neutrality, one can now calculate the density and potential distributions by performing iterative procedures starting with a homogeneous charge distribution at the plane of the 2DES. Note that these quantities should be obtained at each layer of the crystal matrix which requires a huge computational effort. However, the iterative process can be optimized by using successive over relaxation method. Meanwhile, updating the matrix values in each iteration step is minimized by employing the fourth-order grid method which is developed to solve such systems.[20] Once the electrostatic quantities converge numerically, i.e., the density and potential profiles do not change within an accuracy of 10^{-7}, the iteration procedure is halted. We specify the experimental parameters such as the crystal growth parameters and the gate voltages in Sec. III.

B. 2D electron system subject to magnetic field

In the previous step, we have presented the numerical scheme to obtain the charge and potential distributions of the crystal at each layer, including the layer of the 2DES, at zero temperature and in the absence of an external magnetic field. Our next goal is to obtain the same quantities at finite temperatures and in the presence of a high quantizing magnetic field. In principle, we have to solve the same equations given above at the layer of 2DES. Since, the distribution of the positive charges and the charges at the surfaces are approximately unaffected by the finite low temperature (<10 K) and perpendicular B field, we assume that these quantities remain unchanged. However, for the 2DES we have to re-

place the constant DOS by the magnetic field modified one as follows:

$$D(E) = \frac{1}{2\pi l_B^2} \sum_n A_n(E, E_n), \tag{3}$$

where $l_B (= \sqrt{\hbar / eB})$ is the magnetic length. The spectral function $A_n(E, E_n)$ is determined by the disorder, which we discussed in detail in our previous work.[15] The argument of the spectral function depends on the Landau energies $E_n = \frac{\hbar eB}{m^*}(n+1/2)$, with an effective mass m^* and Landau index n. Hence, now one can write the self-consistent equation at the plane of the 2DES (z_0) as

$$\begin{aligned} V(x,y,z=z_0) &= V_{\mathrm{D}}(x,y,z=z_0) + V_{\mathrm{G}}(x,y,z=z_0) \\ &+ \frac{e^2}{\epsilon_{\mathrm{m}} \pi l_B^2} \int \int K(x,y,x',y') \\ &\times \int dE \sum_n A_n(E,E_n) f[E,E_n,V(x,y,z=z_0),T] dx' dy', \end{aligned} \tag{4}$$

where ϵ_{m} is the dielectric constant of the material and $K(x,y,x',y')$ is the solution of the Poisson equation satisfying the boundary conditions. The spatial integration is preformed over the area of the sample, whereas the energy integral and the sum run from 0 to infinity.

The above integral equation is again solved by numerical iteration procedures, namely, by Newton-Raphson, till the desired numerical accuracy is obtained. It is known that the Thomas-Fermi approximation fails, if the potential varies strongly within the quantum mechanical length scales and one should obtain the actual wave functions.[26] Such a failure is also observed in quantized Hall systems[13] and is cured by the inclusion of the finite extends of the wave functions.[21] As mentioned before, it is seemingly difficult to incorporate the wave functions to the calculation scheme, therefore a spatial course-graining procedure is proposed to simulate the quantum mechanical effects.[21,24] This reduces the computational efforts remarkably without scarifying the essential physics. In the following we also perform such a procedure.

The above summarized calculation scheme allows us to calculate the electron-density and electrostatic potential distributions at finite temperature and magnetic field, in a self-consistent manner. The most important outcome of this calculation is that we can calculate the spatial distribution of the current carrying incompressible strips depending on the experimental conditions. As a remark, we would like to note that at the incompressible strips the Fermi energy falls into the single-particle gap locally, where screening is poor. In contrast, the Fermi energy is pinned to one of the Landau levels at the compressible strips and the system behaves like a metal, where screening is nearly perfect and $\sigma_l > 0$ due to finite scattering. In the next section we describe the transport properties of the system at hand utilizing a local version of the Ohm's law.

C. Imposed external current

The transport through a quantized Hall system is commonly described by two seemingly different schemes as follows: (i) the semiclassical transport description, which takes into account Landau-level broadening considering finite collisions. So-called the localization or disorder picture.[27] (ii) The quantum mechanical transport description, which considers a ballistic system and finite tunneling (or scattering) between edge channels and contacts. Known as the Landauer-Büttiker formalism.[7,28] The first description relies on the fact that, for a homogeneous system without boundaries, the gauge invariance argument of Laughlin[29] together with disorder induced broadening and localization can explain the quantization of the Hall and vanishing longitudinal conductances.[27] Such that, the electronic wave functions are localized or extended depending on whether the Fermi energy lies in the single-particle (or mobility) gap or not.[30] It is argued that, due to the gauge invariance, the Hall conductance is a topological invariant and the exponentially small contributions to the longitudinal conductance are suppressed by the extended states in a realistic sample.[31,32] The transport is commonly described by the linear-response theory of Kubo formalism.[32] Since, we will utilize the local version of the Ohm's law later, it is necessary to note that the (exponential) locality of the Hall conductivity is well justified in the above-mentioned works by Niu and Thouless,[30] particularly in Sec. III. The second description disregards collisions in a classical manner that results in dissipation, instead considers perfect one-dimensional (1D) edge states and assumes ballistic transport utilizing the Landauer[33] formalism. Therefore, transport is phase coherent within the linear-response regime. In fact without modifications both descriptions are only valid in the linear-response regime. As pointed above these transport theories are seemingly different, they describe the different aspects of the quantized Hall effect considering different regimes. To be explicit, the disordered and the disorder free systems. The phase coherence in the linear-response regime is described by fairly different approaches, however, lead to very similar results.

Our approach can be considered to lie in the semiclassical description, where we explicitly obtain the conductivities from the self-consistent Born approximation depending on the local electron distribution. Therefore, phase coherence is embedded in the conductivity model used. Such that, since the Fermi energy lies in between the single-particle gap within the incompressible strips, locally, the dissipation is exponentially suppressed and the Hall conductivity is a topological invariant. To remind the one to one correspondence between the classical and the quantum mechanical descriptions of the drift plus cyclotron motion of an electron, we point that the Landau wave functions are nothing but the coherent superpositions of the classical cyclotron orbits.[34]

We describe the transport by a fundamental law, namely, the Ohm's law which we consider to be valid also locally. It is useful to reintroduce[22] the definition of (local) Ohm's law,

$$\nabla \mu^*(\mathbf{r})/e = \mathbf{j}(\mathbf{r}) = \hat{\sigma}(\mathbf{r}) \mathbf{E}(\mathbf{r}), \tag{5}$$

where $\mu^*(\mathbf{r})$ is the position-dependent electrochemical potential, $\hat{\sigma}(\mathbf{r})$ is a two by two tensor describing the local conduc-

tivities, and $\mathbf{j}(\mathbf{r})$ is the local current density together with the local electric field $\mathbf{E}(\mathbf{r})$. The calculation procedure is such: first we obtain the electrostatic properties of the system at total equilibrium (i.e., μ^* is position independent and equals to E_F), then impose a small (compared to equilibrium) electrochemical potential difference between source and drain contacts and recalculate the electron distribution depending on newly calculated total potential. Once local equilibrium condition is satisfied together with the numerical convergence, namely, the potential and electron-density distributions do not change within the numerical accuracy of 10^{-7} in the last iteration, the imposed electrochemical potential difference is increased step by step to the target value. It is important to note that if an external current is imposed, a Hall potential develops and the electronic system responds to this induced potential by the redistribution of the charges, i.e., by screening. Now let us consider three different situations considering the compressibility of a *homogeneous* electronic system. Assume that the system is in a compressible state completely, then the induced electrochemical potential is almost perfectly screened, until the amplitude of the imposed current exceeds linear screening regime.[35] This implies that the response of the electronic system to the imposed current is also linear. Similarly, if the system is completely incompressible the response is still linear, however, in this case screening is fairly poor but linear. The interesting case is when the compressible and incompressible states (strips) coexists, then screening is highly nonlinear even if the imposed current is sufficiently small. The above discussion leads to the conclusion that, there is no genuine linear-response regime of the quantized Hall effect within the plateau regimes where compressible and incompressible regions coexist. Note also that, the linear screening holds locally within the strips. Therefore, the linear-response transport theories are valid locally, however, the response of the global system might be nonlinear. Fortunately, if the imposed current amplitude is sufficiently small the induced Hall potential does not change the electronic (and potential) distribution substantially. Hence one can consider the system at hand to be in the linear-response regime, i.e., $V(x,y,z_0;I=0) \approx V(x,y,z_0;I \neq 0)$. The essentials of the nonlinear transport regime within the screening theory is readily discussed in the literature[22,24] and it predictions are tested successfully by experiments.[36] Our results presented in the next sections consider a very small imposed current, therefore, the density distribution does not change substantially. In other words, we are in the linear-response regime, however, we are not limited to this regime and our results in the nonlinear regime are published elsewhere[15,37] considering different geometries.

III. MODELING OF CONTACTS

In this section we employ the calculation schemes described in the previous sections to calculate the electron and current-density distributions considering metallic contacts. We first summarize the experimental findings reported and use the parameters taken from a generic sample. A schematic presentation of the sample is given in Fig. 1. We initialize our calculation by the sample parameters and use the self-consistent 3D Poisson solver at $T=0$, $B=0$ to obtain initial conditions for our finite temperature and field calculations. Next, we solve self-consistent equations in the absence of an imposed external current using a Gaussian broadened density of states, assuming that the broadening Γ is much smaller than the cyclotron energy ($\Gamma/\hbar\omega_c \sim 0.05$). Finally, we impose a small current to the system from the contacts and calculate the current distribution self-consistently, by updating the electron-density distribution modified by the induced electrochemical potential. Here, we consider two different cases, namely, the low-resistance and high-resistance contacts. The first case is modeled by a homogeneous density gradient in front of the contacts, whereas the later is simulated by in-plane metallic fingers generating inhomogeneous density modulations. Note that a homogeneous compressible state at the front of the contacts responds applied current in a linear manner (good Ohmic contact), meanwhile the inhomogeneous modulation yield a nonlinear response, hence Ohmic behavior is lost.

A. Experimental facts

In spite of the importance of the contacts at 2DESs, it was only recent that systematic investigations revealed the actual material composition at the close vicinity of the contacts.[5] The Weis group found that, the contacts annealed with the Ni/Ge/Au composition has the following properties: (i) the 2DES falls apart from the contacts at the Au-rich regions with an electron depleted region that extends 50–150 nm. (ii) In contrast, at the close proximity of NiGe-rich grains the 2DES can reach up to the metallic region, however with a density gradient till the bulk density n_{el} is reached. The question how the current is injected to this region is answered by a model deduced from temperature-dependent resistance experiments pointing that a very high and thin Schottky barrier is formed at the contact/GaAs interface, hence the injection from the contact to the 2DES is due to tunneling.[5,19] The most striking result of such an experimental finding is that the Büttiker-type edge states cannot equilibrate within the contacts due to an electron poor region just in front of the contacts.[1,19] The Landauer-Büttiker formalism is adequate when considering thin (Schottky) barriers and in the absence of an electron poor region. The Landauer formalism can be extended to thick barrier regime, if no electron poor region exists. However, the electron-density gradient in front of the contacts results in almost full reflection of the Büttiker-type edge states, as depicted in Fig. 1(b).

Hence, experiments show that at all alloyed contacts the Büttiker-type edge states are fully or at best partially reflected by the contacts. In the next sections we provide a model that describes the current injection from low/high-resistance Ohmic contacts based on our semiclassical transport description based on the screening theory, taking into account electron-electron interactions at a mean-field level.

B. Sample properties

In Fig. 1(a) we show schematic presentation of the system at hand. The 2DES lies some 150 nm below the surface, where surface potential is pinned to the midgap of GaAs

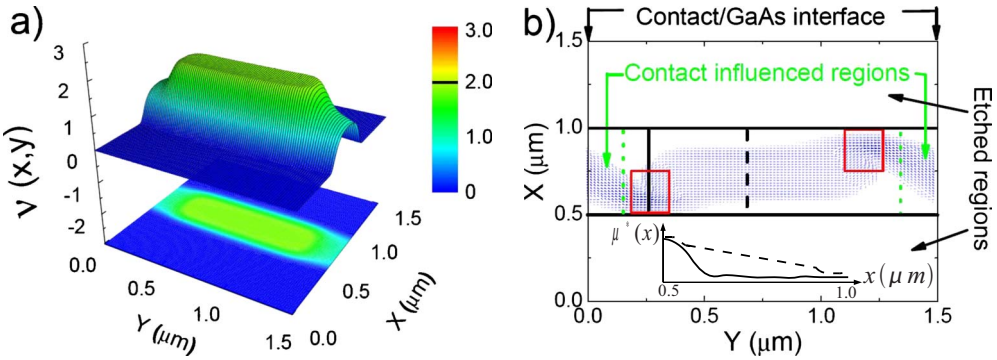

FIG. 2. (Color online) Spatial distribution of the local filling factors $\nu(x,y)$ (a), together with the current density (b) as a function of lateral coordinates. Color scale denotes density gradient, whereas arrows (blue) present the amplitude and direction of the imposed excess current with an amplitude <0.2 nA, guaranteeing linear-response regime. The calculations are performed at $\hbar\omega_c/E_F=4.38$ and default temperature $kT/E_F\sim 0.08$. The electron poor region is a result of metallic contacts at the surface and penetrated metal, kept at −0.5 V. The associated electrochemical potential distributions are shown in the inset of (b), following the vertical solid and broken lines, respectively. Boxes indicate the (hot-)spot regions, separated from the contact regions by broken (green) vertical lines. Here, contact influenced region is defined by the density gradient. The current is injected exactly from $y=0$ μm line exactly at the contact/GaAs interface.

(−0.75 V). Narrow Hall bar is defined by etching at the sides by a depth similar to 65 nm, whereas the metallic fingers reside at the plane of 2DES. To simulate the effects resulting from annealing, we also introduced a metallic region 65 nm below the surface. The contact region is highlighted in Fig. 1(b), where light regions correspond to gold alloy and dark regions represent NiGe alloy. The front of gold alloy is strongly depleted, shown by the white region at the 2DES, whereas, an electron poor stripe resides next to the NiGe alloy. For further references, we define the finger widths (w_f) and lengths (l_f) differently to simulate good ($w_f=0$ nm and $l_f=0$ nm) and bad contacts ($w_f\gtrsim 65$ nm and $l_f\gtrsim 190$ nm). In the case of good contacts we assume that the depleted regions in front of the Au grains are negligibly small. For the bad contacts the depleted region is generated with the metallic fingers by keeping the potential at −0.45 V. The strong confinement in x direction is modified by the contact influenced region.

C. Finite temperature, magnetic field, and current: Low-resistance contacts

We begin our discussion with a case which has a one to one correspondence in *classical* Hall effect: we set the B field such that only the lowest Landau level is partially occupied, hence, behaves like a metal. Throughout this paper, we assume spin degeneracy similar to the previous works[22,24] while the essential physics is independent of the origin of the single-particle gap. However, spin generalized versions of the screening theory already exist.[38,39] It is common to describe the 2D electronic system in the presence of a perpendicular field by a dimensionless parameter; the filling factor ν which measures the occupancy of the Landau levels below the Fermi energy given by the ratio of electron number density $n_{\rm el}$ to the magnetic-flux density n_ϕ. One can express the filling factor also in terms of magnetic length l_B as $\nu=2\pi l_B^2 n_{\rm el}$ and the local version as $\nu(x,y)=2\pi l_B^2 n_{\rm el}(x,y)$. Therefore in this case the filling factor is below 2 (due to spin degeneracy) and there are many available states at the Fermi energy, similar to a metal. Such a case (also locally) is called as compressible, where screening is nearly perfect and electrons can be redistributed according to applied electric fields. Figure 2(a) presents the filling factor distribution (or electron density) calculated for the geometry described above. Such a configuration without metallic fingers at the plane of 2DES mimics a low-resistance (but still reflective) *Ohmic* contact. Due to the strong confinement by the etching, a large electron depleted region resides on both sides of the Hall bar. One observes also that the electronic density is slightly less in front the contacts, compared to the bulk. Note once more that, such a contact with a density poor region is not an ideal contact considering Landauer-Büttiker edge channel picture, as depicted in Fig. 1(b).

1. Classical Hall regime

Let us consider the classical Hall effect first, the current and electrochemical potential distributions are well known:[26] there will be two spots where electrochemical potential is highest (depending on the field direction) at the right-bottom and lowest at the left-top corners. For an illustrative demonstration we suggest the reader to check Fig. 1 of Ref. 8 and also Fig. 4 to compare with actual first principle many-body simulations, performed at the classical regime together with interactions. The experimental findings also support the formation of these spots.[1,40,41] Here the current amplitude is measured in units of $ev_Fk_F/(\pi L_y)$, where v_F and k_F are the Fermi velocity and wave vector, respectively, and L_y (=1500 nm) is the length of the sample, hence the current amplitude is less than 0.2 nA directed in positive y direction. The current distribution also presents two regions where most of the transport takes place, denoted by (red) boxes in Fig. 2(b). We observe that the current is injected homogeneously from the source contact at $y=0$, however, is confined close to the lower corner of the sample. This spot, together with the one near the collector, is called the hot-spot mainly due to the Joule heating caused by confinement of the external current into these small regions. As we will discuss later in detail, formation of these spots occurs by the virtue of

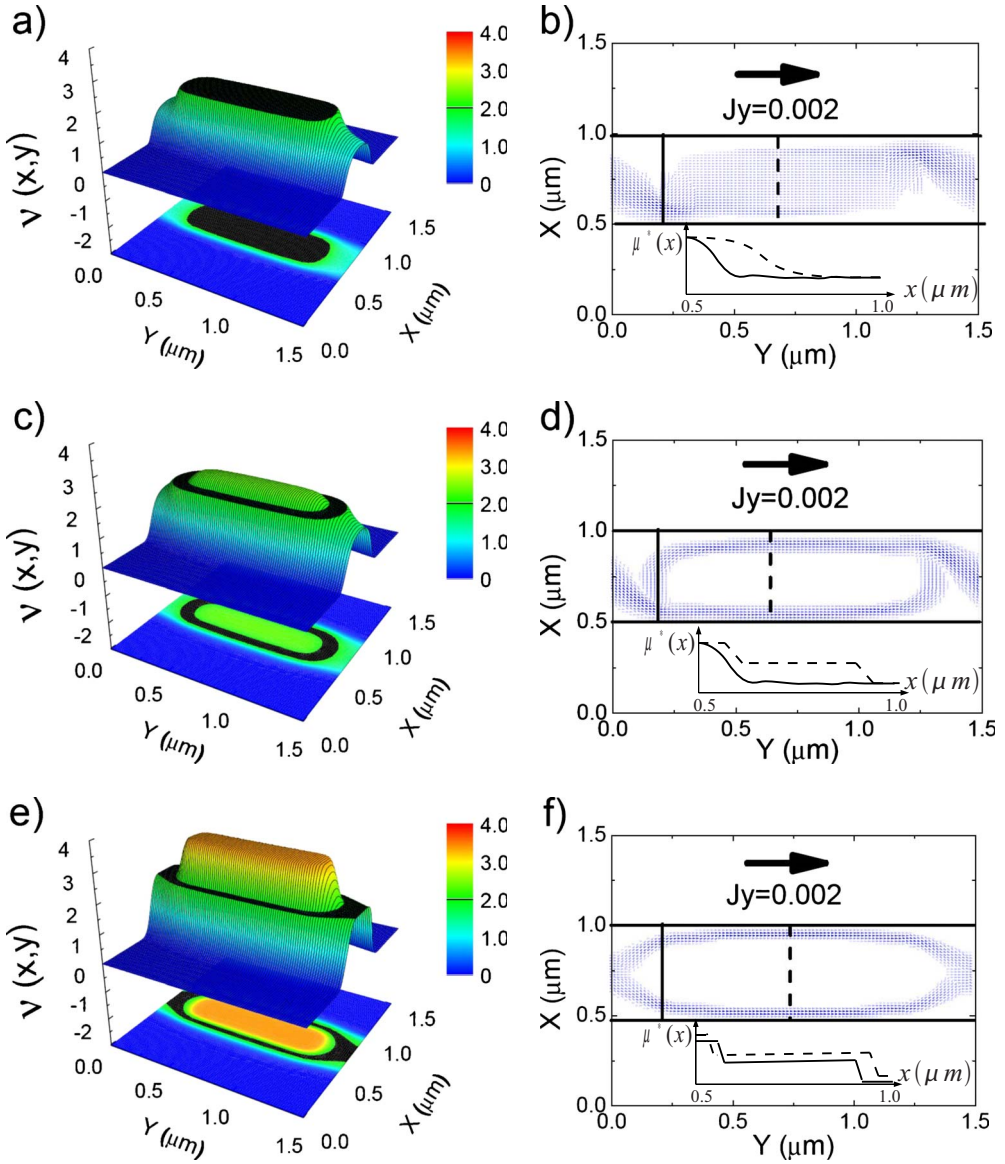

FIG. 3. (Color online) Spatial distribution of the electron densities (left panel) and current densities, same as Fig. 2, calculated at selected B field strengths, [(a) and (b)] $\hbar\omega_c/E_F$=3.78, [(c) and (d)] 3.02, and [(e) and (f)] 2.26 at default temperature. (e) and (f) mimics an ideal contact in edge-channel picture, where no hot-spots are observed. Insets at the right panel demonstrate the electrochemical potential distributions similar to the previous figure.

asymmetric distribution of the Hall potential, even in the linear-response regime. Once the current enters to the bulk of the sample, it is distributed homogeneously following the local electron density, likewise the classical Drude result.[26,42] The classical behavior coincides perfectly with the local probe experiments[2] in the out-of-plateau regime. We also show the demonstrations of the electrochemical potential distribution across the sample in the lower inset of Fig. 2(b). One observes that, the induced potential drops at one of the corners of the sample near the contacts, whereas drops all across the sample when considering the bulk of the sample.

2. Quantized Hall regime

Next, we lower the B field such that a wide incompressible region (denoted by black color) is formed at the bulk of the sample, Fig. 3(a). We also show the corresponding current distribution in Fig. 3(b), where a positive current is imposed in y direction. The (hot)-spots are still visible, however, now the current is injected to the incompressible bulk instead of a compressible bulk. Injecting current to an *incompressible* region is somewhat counter intuitive at a first superficial look. Before elucidating this, we would like to emphasize that our results presented are calculated self-consistently for a given background potential and imposed current. The current is imposed by finite electrochemical potential difference between the source and drain contacts. The spatial distribution of the current density is obtained utilizing the local Ohm's law, where the conductivities are calculated from the local electron-density distribution. Moreover, we do not *assume* that the current should be injected to the incompressible regions. Instead, self-consistency yields such a

case. In fact the key concept is the electrochemical potential difference between contacts: We inject electrons which have an electrochemical potential energy larger than the Fermi energy. Note that, if they were all at the Fermi energy there would be no net total current.

In addition, if one takes into account heating effects[18] due to the high current density at the hot-spots, it is easy to see that the incompressible strips at the injection and collector regions are *melted*, hence the excess current can be transferred between compressible and incompressible regions (and vice versa) easily. Including such local temperature effects are far complicated to be incorporated within our calculation scheme. However, one can still estimate the local electron temperature variation at the hot-spots from the work by Akera, namely, Ref. 18, focusing on Figs. 1 and 2(b) (as a function of filling factor and lattice temperature) or as a function of imposed current amplitude (Fig. 7). Depending on the parameters we employed here, we estimate that, the electron temperature at the hot-spots are 5–10 (and even more in strip case) percent higher than the lattice temperature, which essentially implies that the incompressible region at the hot-spot melts, i.e., the single-particle energy gap closes due to large derivative of the Fermi function. This local heating effect names the spots, i.e., hot-spots, which can also be observed at the linear-response regime. However, the temperature difference may be sufficiently small depending on the imposed current amplitude. In the inset of Fig. 3(b), we also depict the spatial variation in the associated electrochemical potential. It is observed that, at the hot-spot region $\mu^*(x)$ varies in a highly nonlinear manner, having a maximal variation exactly at the spot (solid thick line), whereas, far from the injection contact potential presents an s-shape behavior (broken line) same as the experimental[1] and theoretical[42] findings. Hence, the Hall resistance measured at the center is quantized, however, near the hot-spots deviate from the plateau value considerably. Figures 3(c) and 3(d) correspond to a magnetic field strength where a deformed incompressible ring is formed close to the edges. Nothing different occurs at injector (and collector) region at this B value, the nonlinear potential drop is observed with slight modifications. In contrast the electrochemical potential profile changes substantially at the center, the strong variation only takes place where the incompressible strips reside, inset Fig. 3(e). We observe that, once the current is injected to the incompressible strip it is kept being confined to this region due to the absence of backscattering, till the next hot-spot. One deduces from the electrochemical potential profile that the R_H is quantized, similar to our previous works[24] and experiments.[1]

So far we have observed the features of a reflective, however low-resistance Ohmic contact (nonideal in the language of Landauer-Büttiker) due to the electron poor region in the front of contacts. Our results show that the current can be directly injected to the incompressible strips through the compressible region in front of the contacts. We have seen that, near the contact regions the essential futures of the quantized Hall effect is lost. In contrast, far from the contacts the quantized Hall effect is recovered, we think that these numerical results are in accord with the ones of Ref. 9 and with the experimental findings.[1,5]

Now the question is, what happens if an incompressible edge strip touches the contact region, i.e., an ideal contact. One can roughly estimate the width of the incompressible strip following the nonself-consistent approach proposed by Chklovskii *et al.*[13] in front of the contact as

$$a_1^2 = \frac{16}{\pi} a_B^* l_d [(\nu_0^2 - 1)/\nu_0^2], \tag{6}$$

where, a_1 is the width of first incompressible strip, a_B^* ($\sim$9.81 nm for GaAs/AlGaAs) is the effective Bohr radius, l_d is the depletion length, and ν_0 the bulk filling factor. Note that, in the mentioned work the spin gap equals to the Landau energy (i.e., $\nu=k$ is taken as $1,2,3,\ldots$, however, gap is always $\hbar\omega_c$) and an artificially large strip width is found for odd gaps, misleadingly. To have an ideal contact the incompressible strip in front of the contact should vanish. This requires that, $a_1 \lesssim \lambda_F$ condition has to be satisfied, where λ_F is the Fermi wavelength. For a typical sample, i.e., $\lambda_F \sim 30$ nm and for $\nu_0=1.1$ one observes that the depletion length should be less than 20–30 nm (four to five times the Bohr radius), which is much smaller compared to the experimental findings.[5] Hence, models based on ideal contacts[28,43] has to be revised where the bulk electron density cannot be reach within few a_B^*.

The incompressible strip can extend up to the contact as a natural result of the self-consistency in a very limited magnetic field interval, which we present in Fig. 3(e). The direct Coulomb interaction and Landau quantization (and Lorentz force) pins the electron density just in front of the contact to an (even) integer filling factor at $2.26\hbar\omega_c/E_F^0$. The corresponding, current distribution is shown in Fig. 3(f), where one cannot observe the formation of the hot-spots. Since, all the current is directed along the incompressible strip starting from the injection contact (namely, due to the absence of backscattering). In this case, one can think of a nonreflective contact in the terminology of Landauer-Büttiker edge-state formalism. Unfortunately, such a case is in contrast to the local probe measurements[1] and other experiments which report hot-spots.[40] Therefore, one can conclude that at the alloyed contacts there always exists on irregular density fluctuation.

D. Non-Ohmic contacts

The influence of the contact quality on the quantized Hall effect was also investigated in Refs 5 and 19. It was reported that, measurements performed on deeper lying heterostructures considering contacts which are defined in bad contacting direction, the plateaus are not well developed. In this last part we model *bad contacts*, yet utilizing thick metal fingers residing in the plane of the 2DES, namely, we set the finger length to be 190 nm and width 65 nm, at the injection and collector channels. These metallic fingers essentially represent electronically depleted regions in front of Au grains. Whereas, the Ni/Ge grains correspond to regions in between the fingers (kept at ground). Hence, an inhomogeneous a density gradient occurs. A typical result is shown in Fig. 4, considering same parameters chosen in Figs. 3(e) and 3(f), together with contour lines of the current density. Here, we

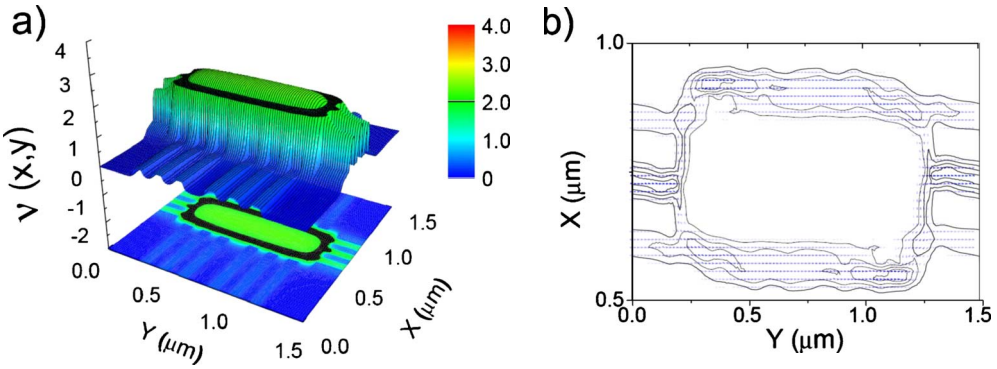

FIG. 4. (Color online) Self-consistently calculated (a) carrier density and (b) current-density distributions, where (b) focuses on the 2DES region. The fluctuations at the contour plot present the anomalies near the contacts, smearing out the quantized Hall effect.

superimposed density fluctuations induced by negatively charged (−0.5 V) metallic fingers to simulate effects resulting from large Au grains, both in the longitudinal (corresponding to injection and collector contacts) and lateral (simulating probe contacts) directions, where latter is defined by thicker fingers (l_f=530 nm and w_f=80 nm). The first observation is that, the current is injected in an inhomogeneous way from the contact to the 2DES, moreover, no incompressible strips form at the inner parts of the fingers due to the strong potential variation. Hence, scattering is enhanced at this field. To simulate the effect of bad side contacts we also impose metallic fingers on the sides. We set the widths and lengths similar to the injection/collector contacts, whereas in Figs. 2 and 3 these lengths were set to zero. We observe that, the density in the lateral direction also presents oscillations and the widths of the incompressible strips vary considerably, even they become narrower than the extent of the wave function. Hence, the backscattering free strips are lost, resulting in nonquantized Hall plateaus. Instead of hot-spots, we see that the current is diverted to the right-bottom corner due to Lorentz force. The influence of bad probe contacts would be suppressed if these side contacts reside far apart. Unfortunately, our numerical abilities are limited by the dimensions of the matrix mapping the Hall bar, therefore we cannot perform systematic investigations in this regime. In any case, our results suggest that, once the density and potential fluctuations imposed by probe contacts are suppressed at large distances the ideal behavior would be recovered. Another important point to note is, once the sample becomes wider and the effect of potential fluctuations are suppressed by screening near the side contacts, the quantized Hall effect would be recovered since one only measures the (electrochemical) potential difference between the side contacts.

IV. CONCLUSIONS

Here, we investigated the influences of contacts on the current and density distributions, considering a Hall bar under quantized Hall conditions, within the screening theory. We modeled the contacts following the ideas put forward by the Weis group based on the experimental findings, namely, the formation of an electron poor region in the close proximity of contacts. It is shown that, in the *classical* regime, where all the system is compressible and behaves like a metal, the well known hot-spots are formed at the corners of the sample. At lower fields, where Landau quantization becomes important, incompressible strips (or regions) are formed and current is injected to these states via hot-spots in the case of reflective and low-resistance Ohmic contacts. Here we also discussed heating effects in a phenomenological manner and argued that due to high current densities at the hot-spots the incompressible regions melt locally. Moreover, we showed that due to the electron poor region, Landauer-Büttiker edge channels are reflected from the contacts and can be considered as nonideal contacts. We also provide numerical results such that if the B field and the contact structure are chosen appropriately, one can still obtain a nonreflective contact in the terminology of Landauer-Büttiker formalism. However, one cannot observe the formation of hot-spots in this case which is in contradiction with the experiments mentioned, unfortunately. In a final discussion, we also simulated bad contacts taking into account potential fluctuations resulting from Au/Ni/Ge alloys by placing metallic fingers in the plane of the 2DES. We observed that, the incompressible strips are destroyed and considerable amount of scattering takes place both near the injection/collector and side probe contacts, hence the quantized Hall effect is lost. Our findings are in accord with the experimental findings and also with the numerical investigations considering the classical regime and nonequilibrium network model. The investigation of actual injection of electrons through the Schottky barrier and local temperature effects demands a more complicated calculation than presented in this work, however, our numerical investigations support the idea that such an investigation might modify the picture presented slightly in a small parameter space.

While submitting our paper, we have encountered a very recent experimental paper reporting on the anisotropic depletion at contact interfaces measured by scanning force microscope.[19] The reported potential profiles strongly support our model, which identifies presence of an incompressible strip in front of Ohmic contacts, that might decouple compressible bulk from the contacts. Moreover, our modeling of good/bad contacts also perfectly agrees with their findings.

ACKNOWLEDGMENTS

We thank to E. Ahlswede, F. Dahlem, and J. Weis for introducing us the scanning force microscope results and for the critical discussions. A. Weichselbaum is acknowledged for sharing his experiences and 3D Poisson solver routine. Fruitful discussions with T. Kramer is also appreciated. We would like to express our gratitude to R. R. Gerhardts, who introduced us most of the concepts of the screening theory. A.S. acknowledges E. J. Heller for giving the opportunity to work in his distinguished group at Harvard University, Physics Department. This work is financially supported by the Scientific and Research Council of Turkey under Grant No. TBAG-109T083 and Istanbul University under Grant No. BAP-6970.

[1] E. Ahlswede, P. Weitz, J. Weis, K. von Klitzing, and K. Eberl, Physica B **298**, 562 (2001).
[2] E. Ahlswede, J. Weis, K. von Klitzing, and K. Eberl, Physica E **12**, 165 (2002).
[3] F. E. Camino, W. Zhou, and V. J. Goldman, Phys. Rev. B **72**, 155313 (2005).
[4] M. Avinun-Kalish, M. Heiblum, O. Zarchin, D. Mahalu, and V. Umansky, Nature (London) **436**, 529 (2005).
[5] O. Goektas, Ph.D. thesis, Stuttgart University, 2009.
[6] R. T. Tung, Mater. Sci. Eng. R. **35**, 1 (2001).
[7] M. Büttiker, Phys. Rev. Lett. **57**, 1761 (1986).
[8] T. Kramer, V. Krueckl, E. Heller, and R. Parrott, Phys. Rev. B **81**, 205306 (2010).
[9] C. Uiberacker, C. Stecher, and J. Oswald, Phys. Rev. B **80**, 235331 (2009).
[10] O. Göktaş, J. Weber, J. Weis, and K. von Klitzing, Physica E **40**, 1579 (2008).
[11] K. v. Klitzing, G. Dorda, and M. Pepper, Phys. Rev. Lett. **45**, 494 (1980).
[12] A. M. Chang, Solid State Commun. **74**, 871 (1990).
[13] D. B. Chklovskii, B. I. Shklovskii, and L. I. Glazman, Phys. Rev. B **46**, 4026 (1992).
[14] K. Lier and R. R. Gerhardts, Phys. Rev. B **50**, 7757 (1994).
[15] S. Arslan, E. Cicek, D. Eksi, S. Aktas, A. Weichselbaum, and A. Siddiki, Phys. Rev. B **78**, 125423 (2008).
[16] A. Siddiki and F. Marquardt, Phys. Rev. B **75**, 045325 (2007).
[17] H. Akera, J. Phys. Soc. Jpn. **69**, 3174 (2000).
[18] S. Kanamaru, H. Suzuuara, and H. Akera, Proceedings of the EP2DS-14, Prague, 2001 [J. Phys. Soc. Jpn. **75**, 064701(2006)].
[19] F. Dahlem, E. Ahlswede, J. Weiss, and K. Klitzing, Phys. Rev. B **82**, 121305(R) (2010).
[20] A. Weichselbaum and S. Ulloa, Phys. Rev. E **68**, 056707 (2003).
[21] A. Siddiki and R. R. Gerhardts, Phys. Rev. B **70**, 195335 (2004).
[22] K. Güven and R. R. Gerhardts, Phys. Rev. B **67**, 115327 (2003).
[23] T. Ando, A. B. Fowler, and F. Stern, Rev. Mod. Phys. **54**, 437 (1982).
[24] A. Siddiki, EPL **87**, 17008 (2009).
[25] T. Champel, S. Florens, and L. Canet, Phys. Rev. B **78**, 125302 (2008).
[26] N. W. Ashcroft and N. D. Mermin, *Solid State Physics* (Brooks Cole, United States of America, 1976).
[27] B. Kramer, S. Kettemann, and T. Ohtsuki, Physica E **20**, 172 (2003).
[28] B. I. Halperin, Phys. Rev. B **25**, 2185 (1982).
[29] R. B. Laughlin, Phys. Rev. B **23**, 5632 (1981).
[30] Q. Niu and D. J. Thouless, Phys. Rev. B **35**, 2188 (1987).
[31] M. Kohmoto, Ann. Phys. **160**, 343 (1985).
[32] Q. Niu, D. J. Thouless, and Y. S. Wu, Phys. Rev. B **31**, 3372 (1985).
[33] R. Landauer, Phys. Lett. **85A**, 91 (1981).
[34] R. E. Prange and S. M. Girvin, *The Quantum Hall Effect* (Springer, New York, 1987).
[35] A. Siddiki and R. R. Gerhardts, Phys. Rev. B **68**, 125315 (2003).
[36] A. Siddiki, J. Horas, D. Kupidura, W. Wegscheider, and S. Ludwig, New J. Phys.(to be published).
[37] A. Siddiki, D. Eksi, E. Cicek, A. Mese, S. Aktas, and T. Hakioğlu, Physica E **40**, 1217 (2008).
[38] A. Siddiki, Physica E **40**, 1124 (2008).
[39] G. Bilgeç, H. Üstünel Toffoli, A. Siddiki, and I. Sokmen, Physica E **42**, 1058 (2010).
[40] R. Knott, W. Dietsche, K. von Klitzing, K. Eberl, and K. Ploog, Semicond. Sci. Technol. **10**, 117 (1995).
[41] W. Dietsche, K. von Klitzing, and K. Ploog, Surf. Sci. **361-362**, 289 (1996).
[42] A. Siddiki and R. R. Gerhardts, Int. J. Mod. Phys. B **18**, 3541 (2004).
[43] M. Büttiker, IBM J. Res. Dev. **32**, 317 (1988).